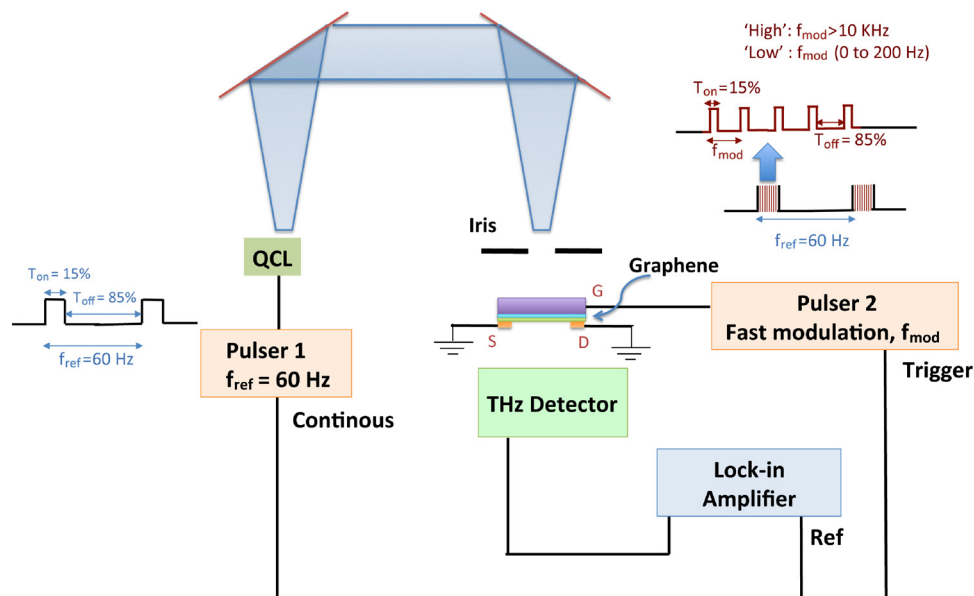


Indirect Modulation of a Terahertz Quantum Cascade Laser Using Gate Tunable Graphene

Volume 4, Number 5, October 2012

Shruti Badhwar
 Reuben Puddy
 Piran R. Kidambi
 Juraj Sibik
 Anthony Brewer
 Joshua R. Freeman
 Harvey E. Beere
 Stephan Hofmann
 J. Axel Zeitler
 David A. Ritchie



DOI: 10.1109/JPHOT.2012.2215312
 1943-0655/\$31.00 ©2012 IEEE

Indirect Modulation of a Terahertz Quantum Cascade Laser Using Gate Tunable Graphene

Shruti Badhwar,¹ Reuben Puddy,¹ Piran R. Kidambi,² Juraj Sibik,³
Anthony Brewer,¹ Joshua R. Freeman,⁴ Harvey E. Beere,¹
Stephan Hofmann,² J. Axel Zeitler,³ and David A. Ritchie¹

¹Department of Physics, University of Cambridge, U.K.

²Center for Advanced Photonics and Electronics, University of Cambridge, U.K.

³Department of Chemical Engineering, University of Cambridge, U.K.

⁴Laboratoire Pierre Aigrain, Paris, France

DOI: 10.1109/JPHOT.2012.2215312
1943-0655/\$31.00 ©2012 IEEE

Manuscript received July 11, 2012; revised August 16, 2012; accepted August 19, 2012. Date of publication August 24, 2012; date of current version September 10, 2012. Corresponding author: S. Badhwar (e-mail: sb732@cam.ac.uk).

Abstract: We bring together two areas of terahertz (THz) technology that have benefited from recent advancements in research, i.e., graphene, a material that has plasmonic resonances in the THz frequency, and quantum cascade lasers (QCLs), a compact electrically driven unipolar source of THz radiation. We demonstrate the use of single-layer large-area graphene to indirectly modulate a THz QCL operating at 2.0 THz. By tuning the Fermi level of the graphene via a capacitively coupled backgate voltage, the optical conductivity and, hence, the THz transmission can be varied. We show that, by changing the pulsing frequency of the backgate, the THz transmission can be altered. We also show that, by varying the pulsing frequency of the backgate from tens of Hz to a few kHz, the amplitude-modulated THz signal can be switched by 15% from a “low” state to a “high” state.

Index Terms: Graphene, terahertz (THz), quantum cascade laser (QCL), modulator.

1. Introduction

Graphene, a single layer of carbon atoms arranged in a honeycomb lattice, is an extremely attractive material for terahertz (THz) optics. It exhibits a linear energy–momentum relationship, which allows for broadband applications. The plasmonic excitations in graphene are described by massless Dirac fermions where the plasmon frequency varies as a function of $N^{1/4}$ as compared with $N^{1/2}$ in conventional semiconductor systems. Here, N is the charge carrier density. These plasmons can be amplified by coupling to intraband transitions, enabling stimulated emission at THz frequencies [1]. The plasmon frequency can be further tuned to resonance by patterning graphene into microribbons allowing manipulation of THz radiation by graphene-based metamaterials [2]. Recently, THz notch filters have been demonstrated in graphene/insulator/graphene microdisks [3]. In the field-effect transistor (FET) configuration, graphene can also act as a photodetector, where the incident THz radiation is rectified and a dc voltage appears across the source–drain electrodes [4].

In this paper, we demonstrate a graphene-based THz modulator operating at room temperature, which can be used to control the transmission from a quantum cascade laser (QCL) emitting at 2.0 THz. QCLs are compact unipolar electrically driven lasers that are currently cited as one of

the most promising sources of THz radiation with applications in ultrafast spectroscopy, non-destructive testing, communications, security screening, and biomedical imaging [5]. QCLs rely on intersubband transitions in multiple quantum-well heterostructures to achieve generation and light amplification by electrical pumping. Progress in QCLs over the past few years has led to sources that are broadband (up to 1 THz bandwidth) [6] and powerful (248 mW) [7], and can operate at temperatures up to 200 K [8]. Previous means of modulating the transmission of a THz QCL relied on direct modulation of the bias voltage by application of an RF signal (up to a few GHz) together with a dc bias [9]. External THz QCL modulators based on electrically driven active metamaterial structures fabricated on semi-insulating GaAs have been reported in the past, with modulation depth $\sim 60\%$ [10]. This paper builds on the recent demonstration of a large-area graphene-based modulator that can be used to manipulate carrier frequencies ~ 570 – 630 GHz [11]. Theoretically, it is possible to achieve modulation depth $< 90\%$ with a graphene-based modulator [12]. THz transmission through graphene is a function of its conductance, i.e., available density of states for intraband transitions [13], [14]. On tuning the Fermi level (E_F) of graphene with an applied gate voltage, the conductivity $\sigma(\omega)$ and, hence, the THz transmission of the graphene $T(\omega)$ referenced to the Si/SiO₂ substrate $T_s(\omega)$ can be controlled as

$$T(\omega)/T_s(\omega) = |(1 + Z_o \cdot \sigma(\omega)/(n_s + 1))|^{-2} \quad (1)$$

where n_s is the refractive index of the silicon substrate (~ 3.41), and Z_o is the vacuum impedance (376.7Ω) [15].

Previous work on broadband modulation [11] relied on Schottky-diode detection of the amplitude-modulated carrier frequency signal from “high” to “low” by switching the applied gate voltage on graphene over millisecond time scales. However, in the frequency range of 1–5 THz, switching of amplitude-modulated THz signals is difficult to detect in time, primarily because of the slow response (4–300 Hz) of the available THz detectors. In this paper, we record the modulated THz transmission by sweeping the frequency of the applied gate voltage (f_{mod}) on graphene while applying a second slow modulation to the QCL (f_{ref}). The response is detected by measuring the average THz power as P_{avg} , where

$$P_{\text{avg}} = P_{\text{peak}}(f_{\text{mod}}) \cdot f_{\text{ref}}/f_{\text{mod}}. \quad (2)$$

The average THz power is switched from a “high” to “low” state by switching the frequency of the backgate voltage on graphene from high ($f_{\text{mod}} > f_{\text{cutoff}}$) to low ($f_{\text{mod}} < f_{\text{cutoff}}$).

2. Experimental Details

The large area (10 mm \times 10 mm) single-layer graphene used in our studies was grown on a copper substrate via chemical vapor deposition (CVD). The copper was subsequently etched, and the graphene film transferred onto a doped Si wafer covered with 300-nm-thick SiO₂ layer. Ti/Au electrodes were evaporated to form the source and drain contacts. The doped Si formed the backgate for the graphene device [see Fig. 1(a)]. Mobilities of up to $\sim 3000 \text{ cm}^2/(\text{V} \cdot \text{s})$ were extracted from Hall bar measurements [16], [17]. The graphene was confirmed as monolayer by Raman spectroscopy [see Fig. 1(b)].

The graphene was first characterized for its broadband response. Fig. 2 shows the THz time-domain spectroscopy (TDS) measurements on large-area graphene biased at different gate voltages. The measurements were done in a dry atmosphere (N_2 purged) at room temperature. An ultrafast femtosecond (12 fs) pulse laser, with a repetition rate of 80 MHz, incident on a photoconductive antenna is used as a broadband THz source. The transmitted radiation was detected by electrooptic sampling. The full description of the system can be found elsewhere [18].

The THz power spectrum [see Fig. 2(a)] is obtained by taking a fast Fourier transform of the time domain data [see Fig. 2(b)]. THz transmission of graphene at $\omega = 2.0$ THz as a function of backgate voltage V_{bg} is shown in the magnified trace in the inset in Fig. 2(a). At $V_{\text{bg}} \sim +50$ V, the Fermi level $E_F = \hbar v_F \sqrt{\pi N}$ is close to the Dirac point. Here, $v_F = 10^6$ m/s is the Fermi velocity of charge carriers. At this point ($V_{\text{bg}} \sim +50$ V), the carrier density N and the conductivity σ is at minimum.

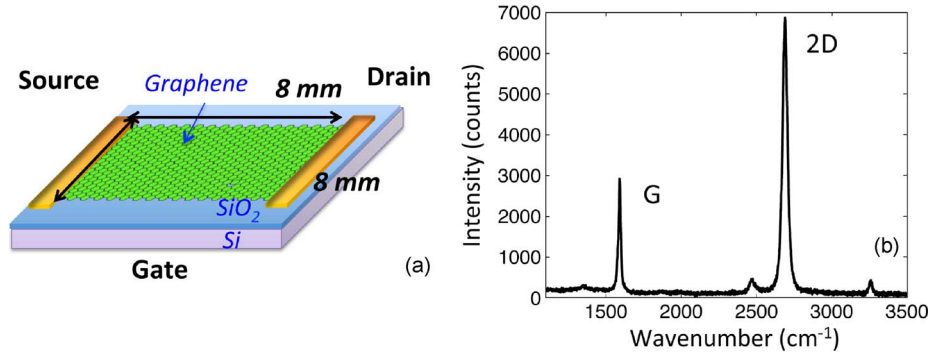


Fig. 1. (a) Device schematic of graphene-based modulator (b) Raman spectroscopy of single-layer graphene.

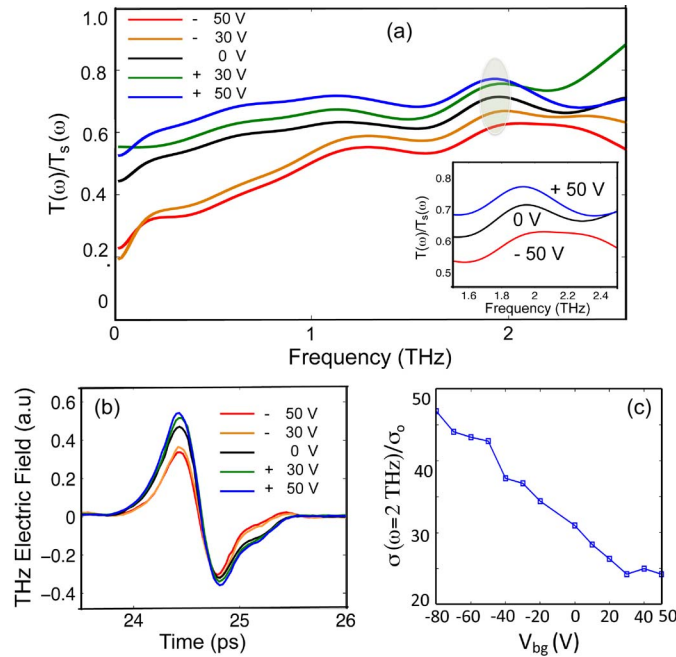


Fig. 2. (a) THz power spectrum normalized to Si/SiO₂ substrate. The inset shows the magnified trace of the transmission through graphene at 2 THz as a function of gate bias (b) THz time-domain signal reflected from the graphene/SiO₂/Si interface (c) AC Conductivity, $\sigma(\omega)$ of graphene normalized to quantum conductivity $\sigma_0 = 2e^2/h$ as a function of backgate voltage.

According to (1), the THz transmission of graphene referenced to that of the Si/SiO₂ $T(\omega)/T_s(\omega)$ is maximum (75%) at this backgate voltage. The transmission falls from 75% (for $V_{bg} = +50$ V) to 70% (for $V_{bg} = 0$ V) to 60% (for $V_{bg} = -50$ V) when the carrier density N is increased by tuning the E_F away from the Dirac point. The optical conductivity $\sigma(\omega)$ increases nonlinearly as expected from theory [14]. Fig. 2(c) shows the ac conductivity as a function of backgate voltage at $\omega = 2.0$ THz. As expected, the ac conductivity as a function of frequency (not shown) follows Drude-like behavior $\sigma(\omega) = iD/\pi(\omega + i\Gamma)$, where Γ is the scattering constant ($\Gamma = 184$ cm⁻¹), and $D = v_F e^2 \sqrt{\pi N}$ is the Drude weight [13]. The dc conductivity determined from the THz transmission spectra as $\sigma_{dc} = D/\pi\Gamma \sim 2.7 \times 10^3 \Omega^{-1}$ agrees with the dc electrical conductivity of graphene determined as $\sigma_{dc} = N\mu e \sim 1.92 \times 10^3 \Omega^{-1}$, where $N \sim 4 \times 10^{12}$ in graphene.

The THz QCL operating at 2.0 THz [Fig. 3(a)] was grown epitaxially on a semi-insulating GaAs substrate in a bound to continuum design [19]. Since the large-area graphene shows a nominally

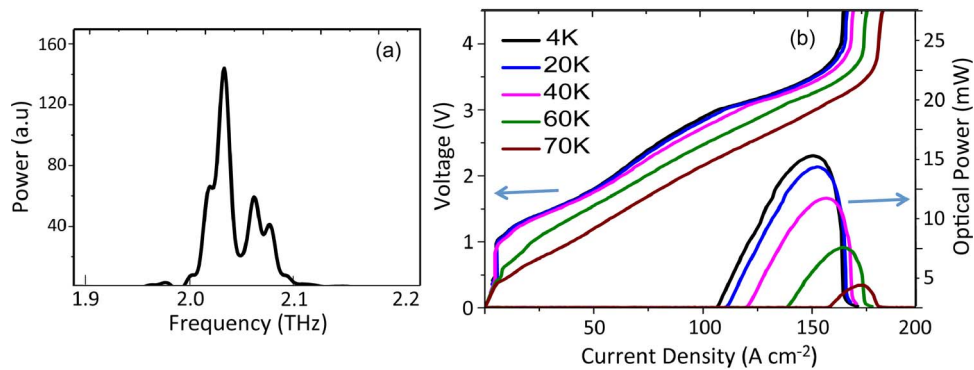


Fig. 3. (a) Spectral characteristics of THz QCL measured using Bruker IFS/66v FTIR spectrometer at $J_{\max} \sim 150 \text{ A/cm}^2$ in the pulsed mode (b) Pulsed LIV of THz QCL at varying temperatures, showing a lasing threshold of 110 A/cm^2 at 4.2 K.

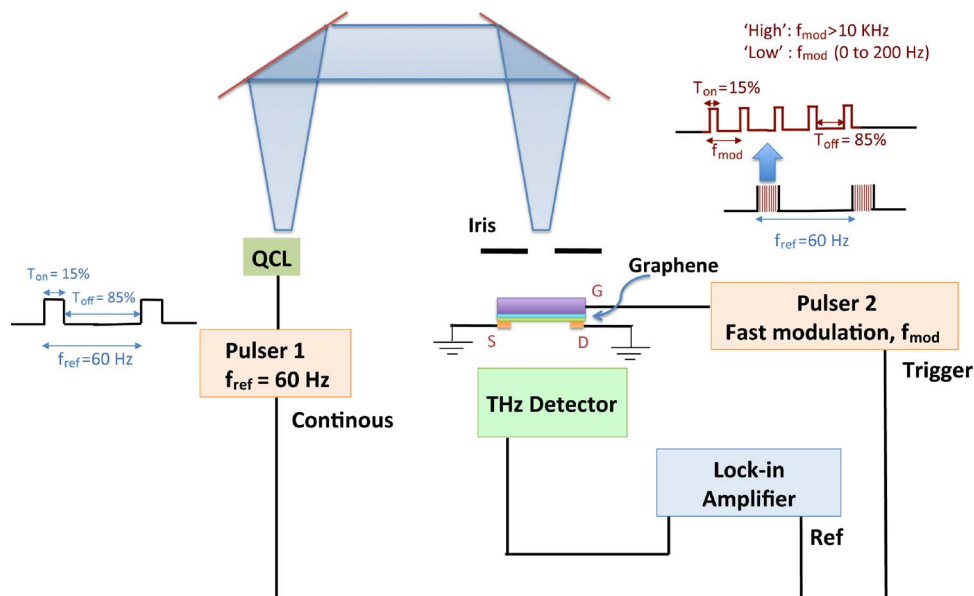


Fig. 4. Experimental Setup. Pulsar 1 provides continuous pulses at 60 Hz, such that the THz QCL operates at J_{\max} in a quasi-cw mode. Pulsar 2 provides a burst of fast modulation to the backgate of graphene.

flat transmission response around 2 THz, it is possible to modulate the THz transmission independently of the operating frequency of the QCL. A $250 \mu\text{m} \times 3 \text{ mm}$ single plasmon waveguide laser was mounted on to a copper block and operated at 4.2 K. In the pulsed mode, the QCL operates up to a maximum temperature of 70 K [see Fig. 3(b)].

The experimental setup is shown in Fig. 4. The QCL biased at $J_{\max} \sim 150 \text{ A/cm}^2$ and is operated in a quasi-cw mode by electrically pulsing at $f_{\text{ref}} = 60 \text{ Hz}$. The duty cycle of this slow pulse is kept at 15%. This envelope frequency (f_{ref}) is applied because most THz detectors operate best at low frequencies. For completeness, we have carried out our experiments with two different THz detectors, i.e., a Golay cell and a composite Si bolometer cryogenically cooled at 4.2 K. To be consistent, we choose $f_{\text{ref}} = 60 \text{ Hz}$ for both measurements. While responsivity of a bolometer is flat for $f_{\text{ref}} < 300 \text{ Hz}$, responsivity of a Golay cell falls by a factor of around seven as the f_{ref} is increased from 15 Hz to 60 Hz. However, the amount of signal detected on the lock-in amplifier for both is well above the noise floor of our measurement setup ($\text{SNR}_{\text{dB}} > 25$). The radiation emitted by the QCL

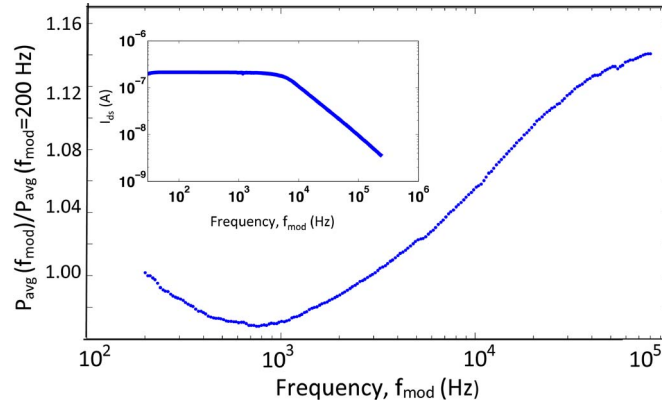


Fig. 5. Average THz power measured as a function of f_{mod} normalized with power at $f_{\text{mod}} = 200$ Hz using a Golay cell at room temperature. The inset shows drain–source current I_{ds} measured as a function of gate modulation at $V_{\text{ds}} = 1$ mV.

source is collected by a pair of F2 parabolic mirrors and is focused onto the THz detector. The graphene-based FET is placed directly in front of the THz detector, at a maximum spacing of 5 mm. The source contact on graphene is grounded. The average THz power is modulated by changing the pulse frequency applied to the backgate of graphene. The backgate is pulsed from 0 to +50 V at a frequency that we denote as f_{mod} . The duty cycle for this pulse is kept at the same value as for the f_{ref} . The modulated signal is measured as the average THz power P_{avg} carried in the 60-Hz envelope on the lock-in amplifier. For better alignment, the beam spot can be further reduced by placing an aperture in front of graphene. We note that the modulation depth is independent of fluence of the incident beam, varied from 60 mW/cm² to 360 mW/cm².

3. Results and Discussion

Fig. 5 shows the measured THz response as a function of f_{mod} , detected by a Golay cell. The pulsing frequency f_{mod} is swept from 200 Hz to 80 kHz. The average detected THz power P_{avg} is normalized to the average detected power at the initial modulation frequency $f_{\text{mod}} = 200$ Hz. The signal is averaged over 10 scans. As mentioned previously, the determination of modulation efficiencies of graphene-based 1–5 THz modulators is limited by the slow response of the available THz detectors. It is for this reason that we vary the backgate voltage frequency f_{mod} and measure the average detected power. Varying the frequency on the gate changes the time period of the THz power transmitted from graphene.

We observe that the average THz power (P_{avg}) detected by the Golay first falls to a certain minimum at $f_{\text{mod}} = f_{\text{cutoff}}$, which is the cutoff frequency. This is where the drain source current I_{ds} (see inset in Fig. 5) remains constant. Note that I_{ds} is given by the following equation for a standard MOSFET, where W and L are the width and length of the graphene channel and ν_{sat} is the saturation velocity:

$$I_{\text{ds}} = q\mu W \frac{\int_0^{V_{\text{ds}}} N dV}{L - \mu \int_0^{V_{\text{ds}}} 1/\nu_{\text{sat}} dV}. \quad (3)$$

According to (1), the peak THz power P_{peak} , transmitted through graphene below the cutoff remains constant. However, the time period of the transmitted power is changed because of the change in f_{mod} . The detector then measures the average power which varies inversely with f_{mod} (2). The drain–source current starts to roll off at $f_{\text{3dB}} = 10$ KHz. This rolloff is explained by the capacitance of the large area SiO₂ gate, at which point the carrier density N induced by the gate falls. Therefore, at this point, the transmitted THz power through graphene, i.e., P_{peak} increases. Note that (1) and (3) suggests that the transmitted power is proportional to I_{ds}^{-2} . The average THz power P_{avg} detected by

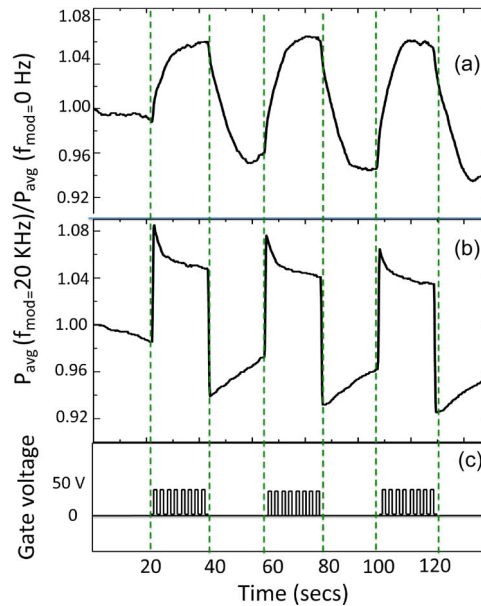


Fig. 6. Amplitude modulated THz signal recorded with time on (a) Golay cell at room temperature (b) composite Si bolometer cryogenically cooled to 4.2 K. The last pane (c) shows the switching of f_{mod} from 0 Hz to a 20-s burst of 20-kHz pulses.

the Golay starts to increase in spite of the inverse dependence on frequency. For an $f_{\text{mod}} = 80$ KHz, the depth of modulation is observed to be $\sim 15\%$.

Fig. 6 shows the amplitude-modulated THz signal as function of time. The graphene is switched from $V_{\text{bg}} = 0$ V, $f_{\text{mod}} = 0$, to a 20-s burst of high frequency pulses ($V_{\text{bg}} = 0$ to +50 V, $f_{\text{mod}} = 20$ KHz). In the first 20 s, $f_{\text{mod}} = 0$ and the transmission through graphene is in the “low” state. In the next 20 s, $f_{\text{mod}} = 20$ KHz and the transmission increases by $\sim 7\%$, corresponding to the normalized $P_{\text{avg}}(f_{\text{mod}} = 20 \text{ KHz})$ (see Fig. 5). However, it can be seen that the measured signal is limited by the response time of Golay [see Fig. 6(a)]. When the same experiment was repeated using a bolometer [see Fig. 6(b)], the speed of response improves by a factor of 1000. We also observe an overshoot and then decay of the THz signal, which we believe is independent of the bolometer’s response time. This transient behavior arising possibly because of device parasitic capacitance or photocurrent saturation is not yet fully understood and is under investigation.

We observe that an improvement of a factor of 2 can be made by operating the graphene between ± 50 V (a voltage limitation on our pulser). Another handle on improving the modulation depth is possibly via chemical doping of graphene, with increase in N to $\sim 10^{14} \text{ cm}^{-2}$ with an ionic gel instead of a backgate. The frequency f_{cutoff} depends on the RC time constant of the graphene device and can be potentially increased from a few kHz to a few MHz by reducing the size of graphene down to the THz beam spot size ($0.5 \text{ mm} \times 0.5 \text{ mm}$). It might also be possible to achieve THz modulation at $\sim \text{GHz}$ frequencies by using an array of high-frequency graphene FETs [20]. Theoretically, the modulation depth can also be increased by employing multiple graphene layers stacked on top of each other, separated by an insulator [3], [11]. In this type of device architecture when one layer is biased at the Dirac point and the other layer is biased away from the Dirac point, it is possible to achieve a THz transmission nearing zero. It is also possible to achieve a narrow-band metamaterial-based modulator in graphene by patterning graphene into microribbons [2]. On tuning the graphene in and out of plasmon resonance by changing the carrier concentration, the transmission can be switched from “high” to “low.” All these separate approaches suggest that there still remains an opportunity to optimize and design a highly efficient compact graphene-based THz modulator.

4. Conclusion

We have shown that the THz power from a QCL can be modulated by applying a gate pulse to large-area CVD-grown graphene. The average THz power measured on the detector increases with increase in pulsing frequency f_{mod} after a certain cutoff. The f_{cutoff} , which is function of the intrinsic RC time constant, corresponds to the rolloff in graphene conductance. The THz signal can be amplitude modulated from a “low” to a “high” state, by switching the backgate voltage on graphene from 0-V dc (or $f_{\text{mod}} < f_{\text{cutoff}}$) to a high frequency pulse, with $f_{\text{mod}} > f_{\text{cutoff}}$.

Acknowledgment

We would like to thank Dr. R. Deg’Innocenti for useful discussions and help with experiments.

References

- [1] F. Rana, “Graphene terahertz plasmon oscillators,” *IEEE Trans. Nanotechnol.*, vol. 7, no. 1, pp. 91–99, Jan. 2008.
- [2] L. Ju, B. Geng, J. Horng, M. M. Caglar Girit, Z. Hao, H. A. Bechtel, X. Liang, A. Zettl, Y. R. Shen, and F. Wang, “Graphene plasmonics for tunable terahertz metamaterials,” *Nat. Nanotechnol.*, vol. 6, no. 10, pp. 630–634, Oct. 2011.
- [3] H. Yan, X. Li, B. Chandra, G. Tulevski, Y. Wu, M. Freitag, W. Zhu, P. Avouris, and F. Xia, “Tunable infrared plasmonic devices using graphene/insulator stacks,” *Nat. Nanotechnol.*, vol. 7, no. 5, pp. 330–334, Apr. 2012.
- [4] L. Vicarelli, M. Vitiello, D. Coquillat, A. Lombardo, A. Ferrari, M. P. W. Knap, V. Pellegrini, and A. Tredicucci, “Graphene field effect transistors as room-temperature terahertz detectors,” *Mesoscale Nanoscale Phys.*, Mar. 2012, arXiv: 1203.3232v [cond-mat.mes-hall].
- [5] P. H. Siegel, “Terahertz technology,” *IEEE Trans. Microw. Theory Tech.*, vol. 50, no. 3, pp. 910–928, Mar. 2002.
- [6] D. Turcinkova, G. Scalari, F. Castellano, M. I. Amanti, M. Beck, and J. Faist, “Ultra-broadband heterogeneous quantum cascade laser emitting from 2.2 to 3.2 THz,” *Appl. Phys. Lett.*, vol. 99, no. 19, pp. 191104-1–191104-3, Nov. 2011.
- [7] B. Williams, Q. H. S. Kumar, and J. Reno, “High-power terahertz quantum cascade lasers,” *Electron. Lett.*, vol. 42, no. 2, pp. 89–91, Jan. 2006.
- [8] S. Fatholouloumi, E. Dupont, C. Chan, Z. Wasilewski, S. Laframboise, D. Ban, A. Mátyás, C. Jirauschek, Q. Hu, and H. C. Liu, “Terahertz quantum cascade laser operating up to ~200 k with optimized oscillator strength and improved injection tunneling,” *Opt. Exp.*, vol. 20, no. 4, pp. 3866–3876, Feb. 2012.
- [9] S. Barbieri, W. Maineult, S. S. Dhillon, C. Sirtori, J. Alton, N. Breuil, H. E. Beere, and D. A. Ritchie, “13 GHz direct modulation of terahertz quantum cascade lasers,” *Appl. Phys. Lett.*, vol. 91, no. 14, pp. 143510-1–143510-3, Oct. 2007.
- [10] X. G. Peralta, I. Brener, W. J. Padilla, E. W. Young, A. J. Hoffman, M. J. Cich, R. D. Averitt, M. C. Wanke, J. B. Wright, H.-T. Chen, J. F. O’Hara, A. J. Taylor, J. Waldman, W. D. Goodhue, and J. Li, “External modulation of terahertz quantum cascade lasers using electrically-driven active metamaterials,” *Metamaterials*, vol. 4, no. 2/3, pp. 83–88, Aug./Sep. 2010.
- [11] B. Sensale-Rodriguez, R. Yan, M. M. Kelly, T. Fang, K. Tahy, W. S. Hwang, D. Jena, L. Liu, and H. G. Xing, “Broadband graphene terahertz modulators enabled by intraband transitions,” *Nat. Commun.*, vol. 3, no. 780, pp. 1–7, Apr. 2012.
- [12] B. Sensale-Rodriguez, T. Fang, R. Yan, M. M. Kelly, D. Jena, L. Liu, and H. G. Xing, “Unique prospects for graphene-based THz modulators,” *Appl. Phys. Lett.*, vol. 99, no. 11, pp. 113104-1–113104-3, Sep. 2011.
- [13] J. Horng, C.-F. Chen, B. Geng, C. Girit, Y. Zhang, Z. Hao, H. A. Bechtel, M. Martin, A. Zettl, M. F. Crommie, Y. R. Shen, and F. Wang, “Drude conductivity of Dirac fermions in graphene,” *Phys. Rev. B*, vol. 83, no. 16, pp. 165113-1–165113-5, Apr. 2011.
- [14] I. Maeng, S. Lim, S. J. Chae, Y. H. Lee, H. Choi, and J.-H. Son, “Gate-controlled nonlinear conductivity of Dirac fermion in graphene field-effect transistors measured by terahertz time-domain spectroscopy,” *Nano Lett.*, vol. 12, no. 2, pp. 551–555, Feb. 2012.
- [15] H. Choi, F. Borondics, D. A. Siegel, S. Y. Zhou, M. C. Martin, A. Lanzara, and R. A. Kaindl, “Broadband electromagnetic response and ultrafast dynamics of few-layer epitaxial graphene,” *Appl. Phys. Lett.*, vol. 94, no. 17, pp. 172102-1–172102-3, Apr. 2009.
- [16] P. R. Kidambi, C. Ducati, B. Dlubak, D. Gardiner, R. S. Weatherup, M.-B. Martin, P. Seneor, H. Coles, and S. Hofmann, *The parameter space of graphene CVD on polycrystalline Cu*, 2012, submitted for publication.
- [17] B. Dlubak, P. R. Kidambi, R. Weatherup, S. Hofmann, and J. Robertson, “Substrate-assisted nucleation of ultra-thin dielectric layers on graphene by atomic layer deposition,” *Appl. Phys. Lett.*, vol. 100, no. 17, pp. 173113-1–173113-4, Apr. 2012.
- [18] E. Parrott, J. Zeidler, T. Friscic, M. Pepper, W. Jones, G. Day, and L. Gladden, “Testing the sensitivity of terahertz spectroscopy to changes in molecular and supramolecular structure: A study of structurally similar cocrystals,” *Cryst. Growth Des.*, vol. 9, no. 3, pp. 1452–1460, Mar. 2009.
- [19] C. Worrall, J. Alton, M. Houghton, S. Barbieri, H. E. Beere, D. Ritchie, and C. Sirtori, “Continuous wave operation of a superlattice quantum cascade laser emitting at 2 THz,” *Opt. Exp.*, vol. 14, no. 1, pp. 171–181, Jan. 2006.
- [20] Y. M. Lin, C. Dimitrakopoulos, K. Jenkins, D. B. Farmer, H. Y. Chin, A. Grill, and P. Avouris, “100 GHz transistors from wafer-scale epitaxial graphene,” *Science*, vol. 327, no. 5966, p. 662, Feb. 2010.